International Journal of Electrical and
Electronics Engineering Research (IJEEER)
ISSN(P): 2250-155X; ISSN(E): 2278-943X
Vol. 6, Issue 6, Dec 2016, 25-36

TRANS STELLAR
•Journal Publications •Research Consultancy

LED DRIVER USING A CASCADED BOOSTING CONVERTER WITH A TAPPED - INDUCTOR

KI-DU KIM[1] & FEEL-SOON KANG[2]

[1]*Oky Ltd. Co., Anyang Korea, South Korea*

[2]*Department of Electronics and Control Engineering, Hanbat National Univ., Daejeon Korea*

ABSTRACT

In the viewpoint of efficiency and cost in a high power LED lighting system, it is useful to decrease the driving current and the number of LED channels. In order to reduce the driving current, it needs to increase the driving voltage. To meet this requirement, LED lighting driver using a cascaded boosting converter with a tapped-inductor is presented to obtain a high voltage boosting ratio. The proposed LED driver consists of two voltage conversion stages. The first stage configures like a conventional boost converter, and the second stage is designed by using a tapped-inductor. Both stages have a cascaded connection to maximize the voltage boosting ratio between input and output voltage. After theoretical analysis, simulation and experiment are carried out to verify the validity of the proposed LED lighting driver, and compared the voltage boosting ratio with conventional counterparts[1].

KEYWORDS: LED Lighting, Boost Converter, Double Voltage Boost Converter, Tapped-Inductor

Received: Oct 16, 2016; **Accepted:** Nov 10, 2016**; Published: Nov** 15, 2016; **Paper Id.:** IJEEERDEC20163

Original Article

I. INTRODUCTION

Recently, LED lighting market is rapidly increasing with the appearance of a high power LED, which is substituting for glow, fluorescent, halogen, sodium, and other lighting sources. One of the research issues in the high power LED lighting system is to design an efficient LED driving circuit, which can supply higher driving voltage in order to reduce the number of LED channels. Specially, in a case of portable LED lighting system activated by a battery source, the most important mission of dc-to-dc converter is to step a low battery voltage up to a high voltage as possible as it can. The higher LED driving voltage ensures the lower LED driving current and the lower battery voltage with minimum number of battery stacks. This approach improves an electrical and mechanical stability and reliability of the portable LED lighting system.

To obtain a high voltage boosting ratio, various dc-to-dc converter topologies have been introduced in [1]-[13]. The origin of these converters is the traditional boost converter [1]-[3]. In [4], it proposed a double voltage boost converter, which consists of an inductor, three capacitors, three diodes, and a switching device. By adding two diodes and two capacitors to the conventional boost converter, it obtains two times higher voltage boosting ratio than the boost converter. Voltage stress on switching device and diodes reduces two times lower than the boost converter. However, when it applies to LED lighting driver controlled in a current-control mode,

and a duty-ratio of the switching device limits to 50% to increase the stability, it needs an auxiliary voltage boosting circuit to obtain a voltage boosting ratio over four times. So it increases ESR (equivalent series resistance) in capacitors and ESL (equivalent series inductance) in inductor, which results in a drop of efficiency and performance. The same disadvantages are occurred in a cascaded boost converter, which is introduced in [5]. To solve the problem happened under the limitation of duty-ratio at below 0.5, dc-to-dc converter employing a coupled-inductor have been introduced in [7]-[13]. It is a good solution to obtain a high voltage boosting ratio whereas a duty-ratio is limited at 0.5. However, the market still needs higher voltage boosting ratio to enlarge its application areas. To meet the requirement, it proposes a portable LED lighting driver, which is based on cascaded boosting converter employing a tapped-inductor.

II. PROPOSED PORTABLE LED LIGHTING SYSTEM

A. Circuit Configuration

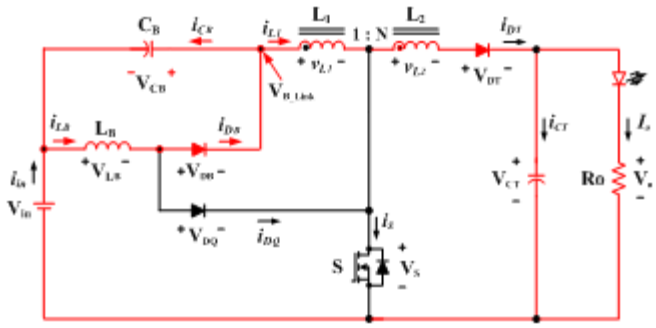

Figure 1: Circuit Configuration of the Proposed Portable LED Lighting System Using a Cascaded Boosting Converter with a Tapped-Inductor

Figure 1 shows a circuit configuration of the proposed portable LED lighting system, which is activated by a battery source. It consists of an input battery with a series-connected capacitor, an input inductor, an output capacitor, three diodes, a switch, and a tapped-inductor. It has two voltage boosting stages. The first stage (Stage-I) configures like the conventional boost converter. The second stage (Stage-II) steps up one more using the turn-ratio of the tapped-inductor. Both voltage conversion stages are connected in series to maximize the voltage boosting ratio. It means that Stage-I generates v_{BLink} and Stage-II steps v_{BLink} up again by using a tapped-inductor. So voltage boosting ratio between input and output voltage is determined by the duty-ratio of a switch (S) and turn-ratio (N) of the tapped-inductor.

B. Operational Modes

In mode analysis, all circuit components are ideal, and ignore stray components. Leakage inductance (L_{lk}) of the tapped-inductor is very small compared with the magnetizing inductance (L_m). V_{in}, V_{BLink}, and V_o are constant. The converter is in a steady-state. The input inductor and tapped-inductor currents are in continuous current conduction mode (CCM). There are two operational modes according to on and off of the switch (S).

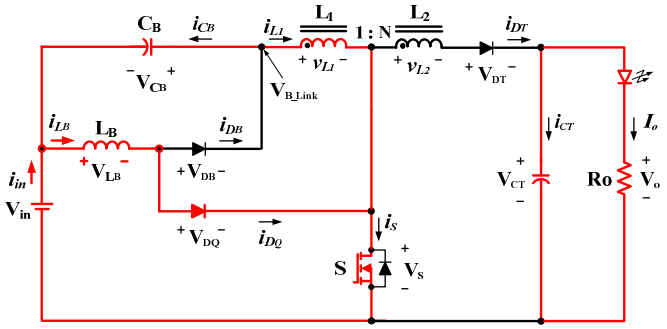

(a)

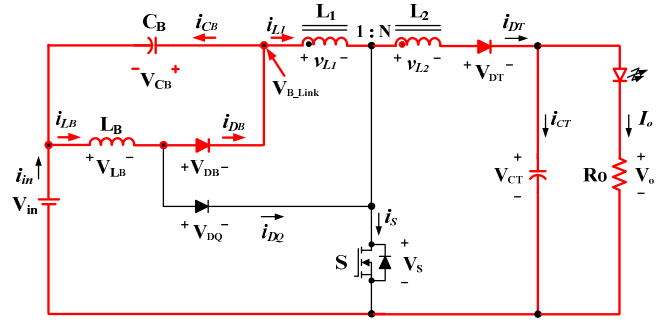

(b)

Figure 2: Operational Modes, (a) Mode 1; *S*=on, (b) Mode 2; *S*=off

Mode 1 ($0<t<DT$): When S turns on, the inductor current (i_{LB}) starts to increase as shown in Figure 2(a). Voltage across the primary winding of the tapped-inductor becomes V_{BLink}, and saves energy in the magnetizing inductance. Here, V_{BLink} is generated by summing of the input battery voltage (V_{in}) and the input capacitor voltage (V_{CB}).

$$V_{BLink} = V_{in} + v_{CB} = V_{in} \cdot \frac{1}{1-D} \tag{1}$$

$$v_{CB} = V_{in} \cdot \frac{D}{1-D} \tag{2}$$

As shown in (1), it has the same relationship between input and output voltage like the conventional boost converter. On the other hand, voltage across the input capacitor (v_{CB}) is like that of buck-boost converter as given in (2). It means that voltage stress on the capacitor C_B can be reduced with the duty-ratio below 0.5 whereas V_{BLink} steps up. During this mode, the output capacitor (C_T) supplies energy to the load.

Mode 2 ($DT<t<T$): When S turns off, the inductor current (i_{LB}) starts to decrease as shown in Figure 2(b). The energy stored in the magnetizing inductance starts to discharge to the load. Here, the output voltage depends on turn-ratio of the tapped-inductor. The input-output voltage relationship with duty-ratio of the switch (S) is delivered by using the voltage-second balancing theory as follows.

$$V_o = V_{in} \cdot \frac{DN+1}{(1-D)^2}. \tag{3}$$

As shown in (3), the output voltage is boosted by not only the duty-ratio of the main switch, but also turn-ratio of the tapped-inductor resulted in higher voltage boosting ratio.

III. DESIGN PROCEDURE

To verify the proposed portable LED lighting system using a battery source of 24V, a prototype of 120W (120V/1A) is manufactured and design procedure is given as follows. Table I lists up the specifications of the prototype. The same parameters are used for simulation and experiment.

Table I: Specifications of Prototype

Parameter	Symbol	Value
Input Voltage (Battery)	V_{in}	24 [V]
Output Voltage	V_o	120 [V]
Output Current	I_o	1 [A]
Input Inductor	L_B	106 [μH]
Tapped-Inductor	L_1, L_2	240 [μH], 960 [μH]
	$N_1 : N_2$	1:2
Capacitor	C_B, C_T	470 [μF]
Switching Frequency	f_s	20 [kHz]

The input battery source is 24V, and maximum supplying current is 18A. For the stable operation of the proposed LED driver, duty-ratio of the switch (S) is limited at 50%.

A. Design of the Tapped-Inductor

When the switch (S) turns off, the secondary of the tapped-inductor starts to flow current via the diode D_T. In this time, the minimum diode current is determined by

$$i_{DT(\min)} = I_o - \frac{\left[V_{in} - V_o(1+D)\right] \cdot N \cdot T}{2 \cdot L_2 \cdot (N+1)} \tag{4}$$

By assuming the current ripple ratio of 50%, the inductance of the secondary of the tapped-inductor is obtained by

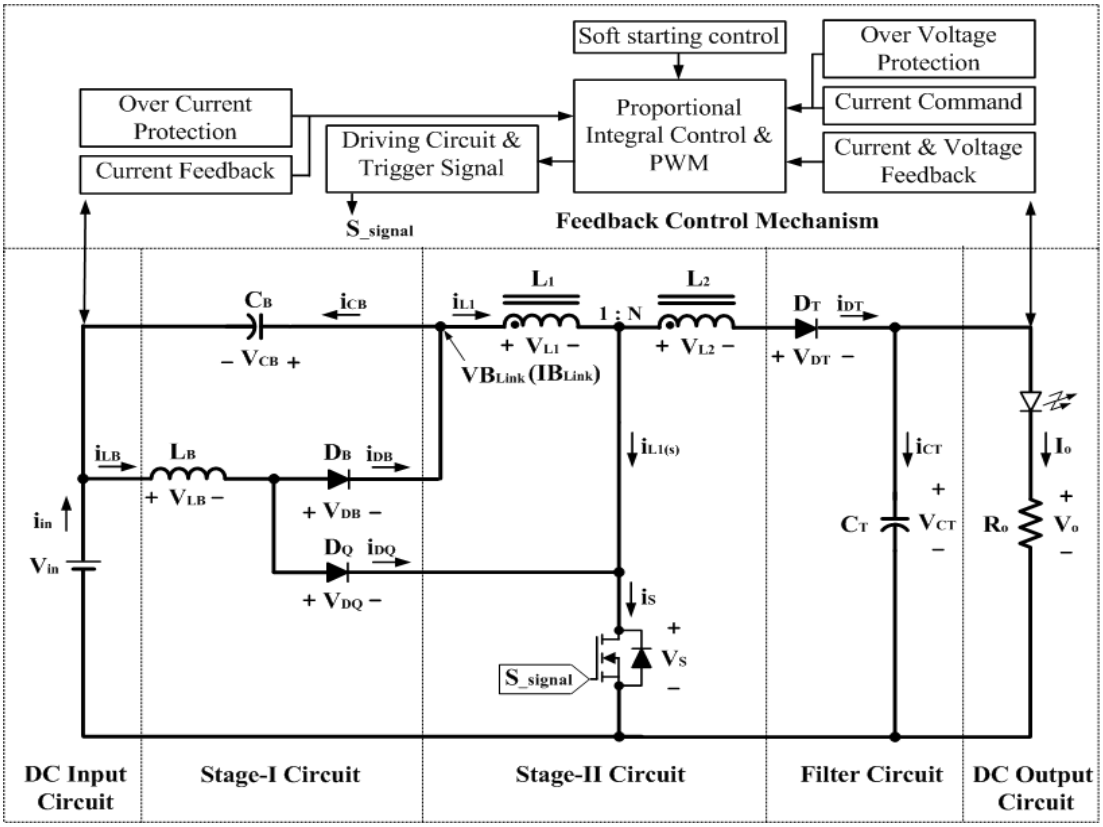

Figure 3: Control Block Diagram for the Proposed Portable LED Lighting System

$$L_2 = \frac{[V_{in} - V_o(1+D)] \cdot N \cdot T}{2 \cdot L_2 \cdot (N+1) \cdot (I_o - i_{DT(\min)})} = 960\mu H \ . \tag{5}$$

Then, the inductance of the primary of the tapped-inductor can be determined by

$$\frac{L_2}{L_1} = \left(\frac{N_2}{N_1}\right)^2 = N^2 \ . \tag{6}$$

Here, the turn-ratio (N) of the tapped-inductor sets to 2. Therefore, the inductance of the primary of the tapped-inductor is given by

$$L_1 = \frac{960 \times 10^{-6}}{2^2} = 240\mu H \ . \tag{7}$$

B. Design of the Input Inductor

The input inductor is designed to be operated in CCM. So the inductance of the input inductor is calculated by

$$L_B = \frac{V_{in} \cdot D \cdot T}{2(I_{LB} - I_{LB(\min)})} = 106\mu H \ . \tag{8}$$

C. Voltage Rating of Diode

When the switch (S) turns on, the diode (D_B) is turned off. In this time, voltage across the diode (v_{DB}) is given by (9) when duty-ratio is limited at 50%.

$$v_{DB(\max)} = -V_{in} - \frac{D \cdot V_{in}}{1-D} = -48V \ . \tag{9}$$

When the switch (S) turns off, the diode (D_Q) is turned off. In this time, voltage across the diode (v_{DQ}) is given by

$$v_{DQ(\max)} = \frac{-V_o + V_{in}(1+D)}{N+1} = -28V \ . \tag{10}$$

When the switch (S) turns on, the diode (D_T) is turned off. In this time, voltage across the diode (v_{DT}) is given by

$$v_{DT(\max)} = -V_o - \left(V_{in} + \frac{D \cdot V_{in}}{(1-D)} \right) \cdot N = -216V \ . \tag{11}$$

D. Voltage Rating of Switch

When the switch (S) turns off, voltage across the switch is given by (12) when duty-ratio is limited at 50%.

$$v_{S(\max)} = \frac{V_o}{(N+1)} + \frac{(2D+N-1)}{(1-D)(N+1)} \cdot V_{in} = -72V \tag{12}$$

The voltage rating of the switch and diodes should be higher than those of given in (9)~(12).

IV. SIMULATION AND EXPERIMENT RESULTS

To verify the validity of the proposed LED lighting driver, simulation and experiments are carried out using the calculated parameters given in Table I. Figure 3 shows a control block diagram of the proposed LED driver. Constant current control algorithm is applied to drive 120W LEDs connected in series.

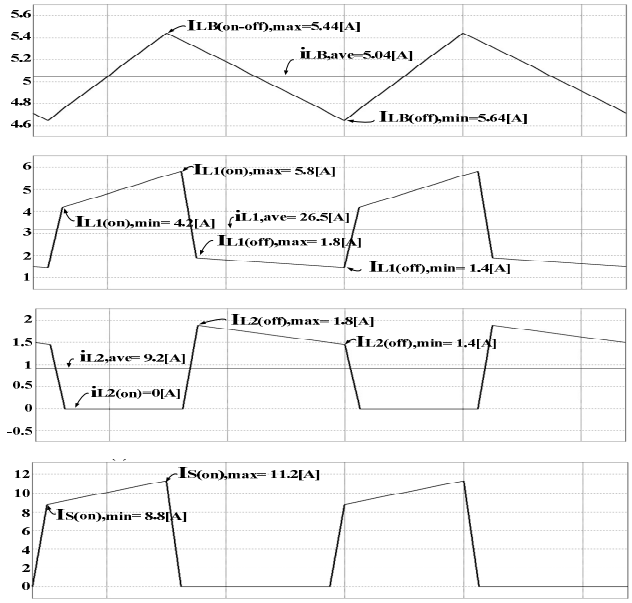

Figure 4: Simulation Results of Inductor Current (i_{LB}), the Primary Current (i_{L1}) and the Secondary Current (i_{L2}) of Tapped-Inductor, Switch Current (i_S) from the Upper to the Lower

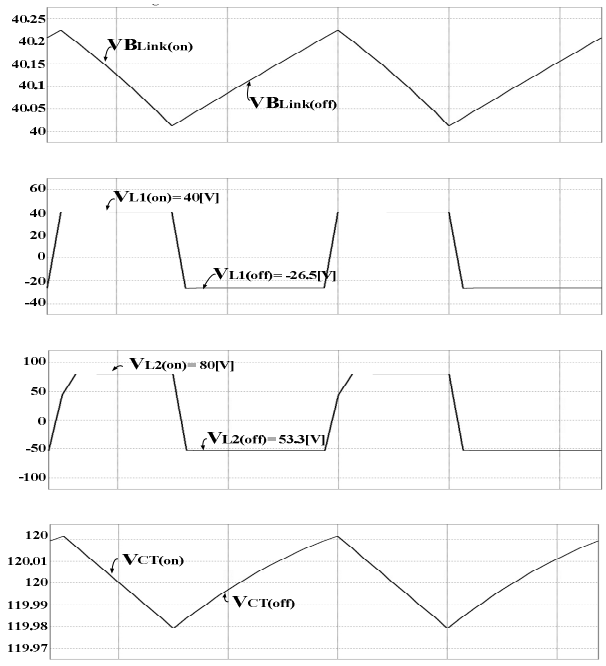

Figure 5: Simulation Results of Terminal Voltage of Stage-I (v_{BLink}), the Primary Voltage (v_{L1}) and the Secondary Voltage (v_{L2}) of Tapped-Inductor, Output Capacitor Voltage (v_{CT}) from the Upper to the Lower

Figure 4 shows simulation results using PSIM. From the upper to the lower, it shows an input inductor current (i_{LB}), the primary current (i_{L1}) and the secondary current (i_{L2}) of tapped-inductor, a switch current (i_S). Figure 5 shows simulation results of a terminal voltage of Stage-I (v_{BLink}), the primary voltage (v_{L1}) and the secondary voltage (v_{L2}) of tapped-inductor, output capacitor voltage (v_{CT}) from the upper to the lower. Maximum, minimum, and average values are depicted on each waveform. Output voltage and load current are shown in Figure 6. Output is 120V and load current is 1A. Both maintain in constant values.

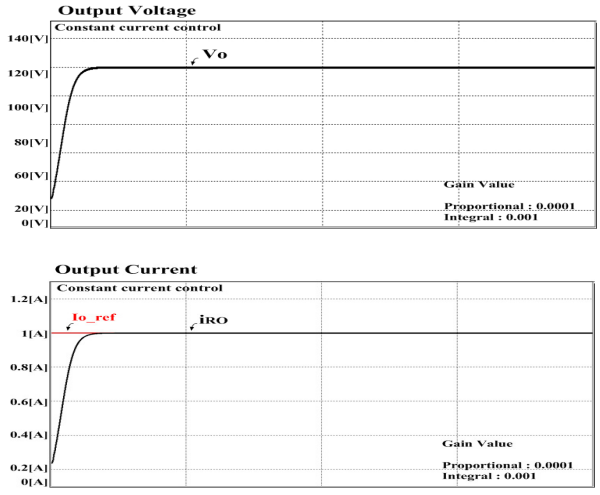

Figure 6: Simulation Results of Output Voltage (v_o) and Output Current (i_{R0}).

Figure 7 shows experiment results based on a prototype. Except surge voltages occurred at switching on/off instant, all waveforms are same with the simulation results. The surge voltage is originated in the leakage inductance of the tapped-inductor. It can be minimized by design optimization of the tapped-inductor and addition of a snubber circuit. Figure 8(a) shows a voltage boosting ratio according to the increase of duty-ratio up to 0.45. It compares with theoretically

calculated, simulated, and experimentally measured values. From the graph, we can notice that three values show a similar tendency. When duty-ratio is 0.2, voltage boosting ratio becomes about 2. When the duty-ratio is 0.4, the voltage boosting ratio becomes over 4.5.

Figure 8(b) shows a voltage boosting ratio according to the increase of turn-ratio of the tapped-inductor. With N=1 and D=0.5, voltage gain is same to the conventional cascaded boost converter introduced in [5]. Both converters can step the output voltage up to four times higher than the input voltage. With the increase of the turn-ratio, the proposed converter sharply increases the slope of voltage gain, but controllable ranges of the duty-ratio become shorter. The reason is that the larger tapped-inductor saves more energy when the switch turns on, but the energy should be demagnetized to prevent saturation of the tapped-inductor. For a perfect reset of the magnetizing energy, the duty-ratio of the switch should be limited at maximum 0.5 below. Theoretically, voltage gain of the proposed converter with N=10 becomes 14 at duty-ratio of 0.4.

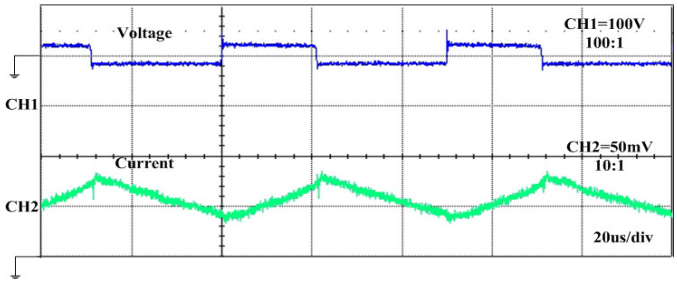

(a)

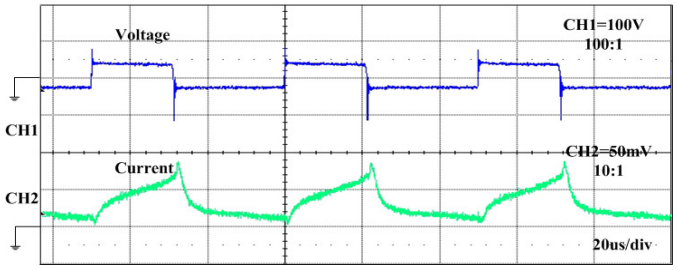

(b)

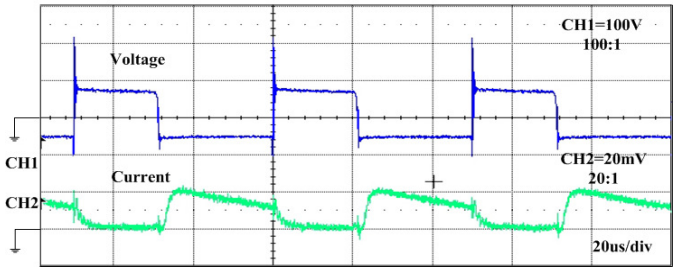

(c)

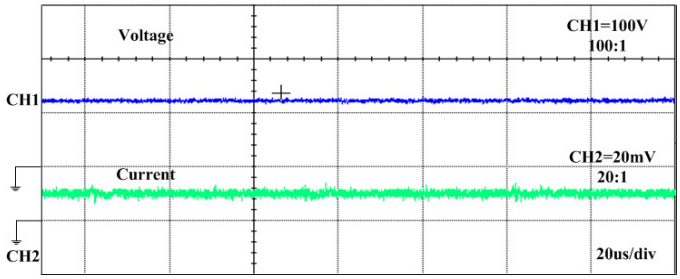

(d)

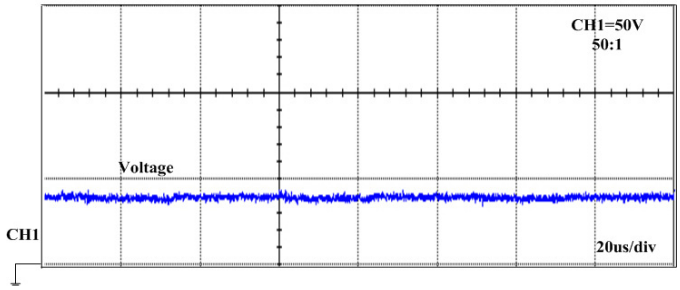

(e)

Figure 7: Experiment Results, (a) Voltage across Inductor L_B (v_{LB}) and Inductor Current (i_{LB}), (b) The Primary Voltage of Tapped-Inductor (v_{L1}) and the Current (i_{L1}), (c) The Secondary Voltage of Tapped-Inductor (v_{L2}) and the Current (i_{L2}), (d) Output Voltage (v_o) and Output Current (i_{R0}), (e) V_{BLink} Voltage

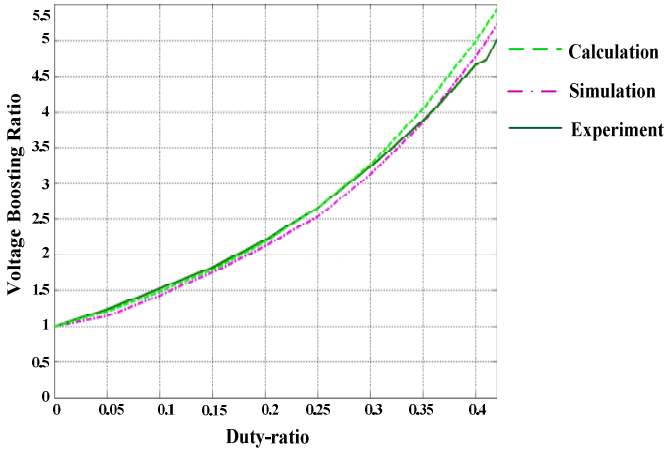

(a)

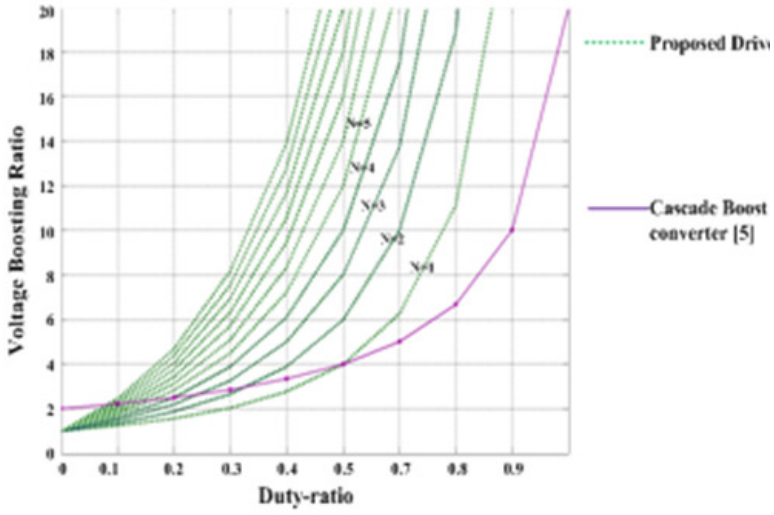

(b)

Figure 8: Variation of Voltage Boosting Ratio, (a) Voltage Gain Due to the Increase of Duty-Ratio, (b) Voltage Gain Due to the Increase of Turn-Ratio

Figure 9 compares voltage boosting ratio with the prior counterparts. The proposed converter can increase the voltage boosting ratio by using duty-ratio and turn-ratio, whereas other counterparts only depends on duty-ratio. In this comparison, turn-ratio of the proposed converter sets to N=2. When duty-ratio is 0.5, the boost converter shows voltage gain of 2. Cascaded boost converter [5] and double voltage boost converter [4] shows voltage gain of 4. Among counterparts, cascaded boost converter employing a coupled-inductor [7] shows the highest voltage gain as 8 like the proposed approach. Here, we can claim that the proposed converter can increase the voltage boosting ratio higher than the cascaded boost converter with a coupled-inductor [7] because the proposed driver can increase turn-ratio of the tapped-inductor.

Table II compares the number of circuit components. The conventional boost converter [3] shows the minimum number of circuit components, however, the voltage boosting ratio is the lowest among counterparts. Although cascaded boost converter employing a coupled-inductor has the same voltage boosting ratio, it needs more circuit components compared to the proposed driver.

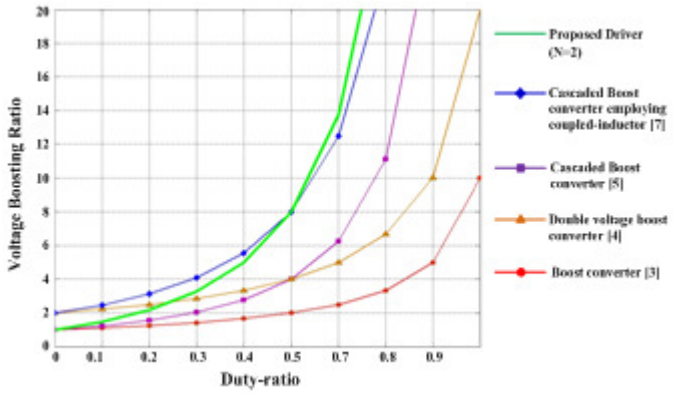

Figure 9: Comparison of Voltage Boosting Ratio with Counterparts

Table II: Comparison of the Number of Circuit Components

	Inductor	Tapped Inductor	Capacitor	Diode	Switch	Total
Proposed driver	1	**1**	2	3	1	8
Boost converter [3]	1	0	1	1	1	4
Cascaded Boost converter [5]	**2**	0	2	3	1	8
Double voltage boost converter [4]	1	0	3	3	1	8
Cascaded Boost converter employing coupled-inductor [7]	**2**	0	**4**	**5**	1	**12**

V. CONCLUSIONS

In this paper, we proposed a portable LED lighting system using a cascaded boosting converter with a tapped-inductor to obtain a high voltage boosting ratio. It consists of two voltage boosting stages, which are connected in series. Stage-I configures like the conventional boost converter, and Stage-II is designed by using a tapped-inductor. Theoretical analysis, simulation, and experiment were implemented to verify the validity of the proposed driver, and compared the voltage boosting ratio and circuit components with four presentable counterparts.

As a result, we can claim that the proposed LED lighting driver can be a good choice for portable LED lighting applications such as camping and emergency lighting at home.

REFERENCES

1. *Erickson, R. W. and Maksimvic. D, Fundamentals of power electronics, John Wiley, 2nd ed., New York, USA, 1950, pp. 39-55.*
2. *Mohan, N. Undeland, T. M and Robbins W. P, Power electronics, John Wiley & Sons Inc., 2nd ed., New York, USA, 1995, pp. 172-178.*
3. *Hart D. W, Introduction to power electronics, Prentice-Hall, New York, USA, 1964, pp. 212-214.*
4. *Luo. F and Ye. H, "Positive output cascade boost converters," in Proc. IEE Electr. Power Appl., vol. 151, pp. 590-606, Sep. 2004.*
5. *Muhammad Aamir, "Design, Implementation and Experimental Analysis of Two-Stage Boost Converter for Grid Connected Photovoltaic System,", in Proc. 3rd IEEE International Conference Computer Science and Information Technology (ICCSIT), vol. 5, pp. 194-199, July 2010.*
6. *Fohriger. J. P and Himmelstoss. F. A, "Analysis of a boost converter with tapped inductor and reduced voltage stress across the buffer capacitor," in Proc. IEEE ICIT, pp. 126-131, Dec. 2006.*
7. *Rong-Jong. Wal and Rou-Yong. Duan, "High step-up converter with coupled-inductor," IEEE Trans. Power Electron., vol. 20, no. 5, pp. 1025-1035, Sept. 2005.*
8. *Jovanovic. M. M. and Yungtaek Jang, "A new soft-switched boost converter with isolated active snubber," IEEE Trans. Ind. Appl., vol. 35, no. 2 , pp. 496-502, Mar. 1999.*
9. *Dong Wang, Yan. Deng, Xiangning. HE, "Designing and Analysis of an interleaved boost converter with passive lossless clamp circuits," in Proc. IEEE IECON, pp. 2149-2155, Nov. 2008.*
10. *Alonso. J. M, Vina. J, Vaquero. D. G, "Analysis and Design of the Integrated Double Buck-Boost Converter as a*

High-Power-Factor Driver for Power-LED Lamps," IEEE Trans. Ind. Electron., vol. 59, no. 4, pp. 1689-1697, Apr. 2012.

11. *Nino Christopher B. Ramos, Miguel T. Escoto Jr, "Design and Analysis of an Interleaved Tapped inductor Boost Converter for Higher Power and Voltage Gain Applications," in Proc. IEEE TENCON, pp. 1-6, Nov. 2012.*
12. *Juan. C. Yris, Jorge H. Calleja, Leobarodo H. Gonzalez, Luis M. Lopez, Rufo P. Martinez, "Analysis of Tapped Inductor Converters in Three Operating Modes for Photovoltaic Systems with Grounded Source," in Proc. 12th International Power Electronics Congress (CIEP), pp. 215-220, Aug. 2010.*
13. *K. I. Hwu, Li-Ling Lee, "Powering LED Using High-Efficiency SR Flyback Converter," IEEE Trans. Ind. Appl., Vol. 47, no. 1, pp. 376-386, Jan. 2011.*

APPENDICES

Ki-du Kim received the B.S. degree in the Department of Control and Instrumentation Engineering from Hanbat National University, Daejeon, Korea in 2011, and the M.S. degree from the same University in 2013. Since 2014, he has been with Oky Ltd. Co. Korea. His research activities are design and control of dc-to-dc converters for LED lighting, on-board charger of electric vehicles. Mr. Kim is a member of KIEE and KIPE.

F. S. Kang received the M.S. and Ph.D. degrees from Pusan National University, Busan, Korea in 2000 and 2003, respectively. From 2003 to 2004, he had been with the Dept. of Electrical Engineering, Osaka University, Osaka, Japan as a Post-doctoral fellow. Since Sept. 2004, he has been with the Dept. of Electronics and Control Engineering, Hanbat National University, Korea as a Professor. From 2012 to 2013, he was with Colorado State University, CO, USA as a Visiting Professor. His research activities are in the area of power electronics including design and control of various power conversion systems for display, renewable energy, electric vehicles, and submarines. He received Award and Prizes from IEEE Industrial Electronics Society. And he was honored Academic Awards from Pusan National University and Hanbat National University in 2003 and 2005, respectively. He also received several Best Paper Awards From KIEE, and KIPE. He served as a vice-chairman of Organizing Committee for Intelec 2009, ICEMS 2010, Maglev 2011, VPPC 2012, ICEMS 2013, and ITEC 2016. He served as an Associate Editor of the IEEE Transactions on Industrial Electronics from 2004 to 2011. Dr. Kang is a member of KIEE, KIPE, and IEEE.